DISCLAIMER NOTICE

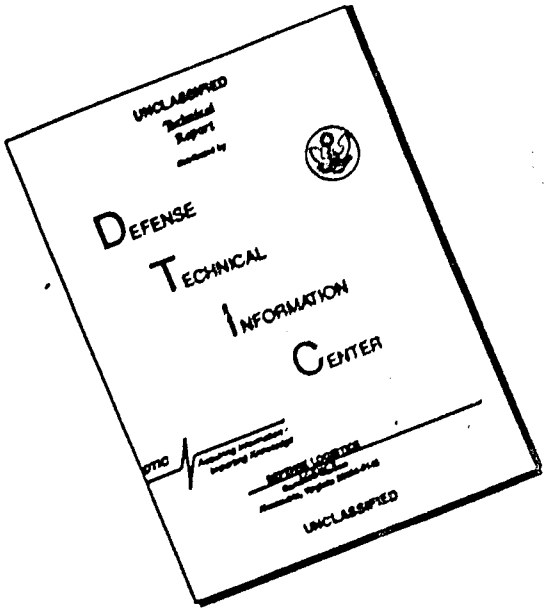

THIS DOCUMENT IS BEST QUALITY AVAILABLE. THE COPY FURNISHED TO DTIC CONTAINED A SIGNIFICANT NUMBER OF PAGES WHICH DO NOT REPRODUCE LEGIBLY.

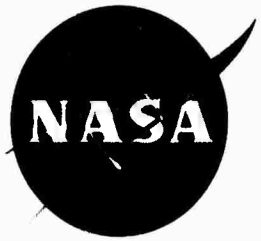

TECHNICAL NOTE
D-851

RELATIONS OF COMBUSTION DEAD TIME TO ENGINE VARIABLES FOR A 20,000-POUND-THRUST GASEOUS-HYDROGEN - LIQUID-OXYGEN ROCKET ENGINE

By Daniel I. Drain, Harold J. Schum,
and Charles A. Wasserbauer

Lewis Research Center
Cleveland, Ohio

NATIONAL AERONAUTICS AND SPACE ADMINISTRATION
WASHINGTON June 1961

NATIONAL AERONAUTICS AND SPACE ADMINISTRATION

TECHNICAL NOTE D-851

RELATIONS OF COMBUSTION DEAD TIME TO ENGINE VARIABLES FOR A 20,000-POUND-THRUST GASEOUS-HYDROGEN - LIQUID-OXYGEN ROCKET ENGINE

E-1269

By Daniel I. Drain, Harold J. Schum,
and Charles A. Wasserbauer

SUMMARY

An uncooled 20,000-pound-thrust gaseous-hydrogen and liquid-oxygen rocket engine was experimentally investigated over a range of chamber pressure from 45 to 300 pounds per square inch absolute and over a range of oxidant-fuel ratio from 2 to 7. Combustion dead times (i.e., the time lag for a change in the oxygen dome pressure to be observed in the combustion-chamber pressure as the oxygen flow rate is abruptly decreased) were measured and were calculated from chamber-pressure frequency measurements for assumed combustion models. One model considered the dead time to be equal to the inverse of twice the observed chamber-pressure frequency. The second model considered the same mathematical expression with the measured frequencies adjusted to compensate for chamber-pressure dynamics in terms of gas residence time. All dead times were correlated to engine operating variables, and it was found that dead time decreased with increasing chamber pressure at constant oxidant-fuel ratio or liquid-oxygen injection velocity. Correspondingly, the dead time decreased with decreasing oxidant-fuel ratio at constant chamber pressure or oxygen injection velocity. Close agreement was obtained between measured dead times and those calculated from frequency measurements corrected for engine dynamics, indicating that combustion dead time, for control purposes, can adequately be determined from chamber-pressure frequency measurements.

INTRODUCTION

Combustion-chamber dynamics are of importance to liquid-propellant rocket-engine designers mainly because of the destruction often attending combustion instability and other vibrations. In addition, with the current interest in space travel, a more thorough knowledge of combustion-chamber dynamics is needed for engine control that will meet

the strict trajectory requirements. An important factor affecting combustion-chamber dynamics is the time lag that exists between propellant injection and combustion. Numerous theoretical studies of combustion dynamics have been made in which this time lag, the dead time, was considered to be dependent upon rocket-engine operating parameters. In reference 1, dead time is related to chamber pressure, while in reference 2 it is related to injection velocity as well.

The purpose of this investigation was to determine experimentally the relation of dead time to the operating parameters of an uncooled hydrogen-oxygen rocket engine of the 20,000-pound-thrust class. Combustion dead times were measured by abruptly decreasing the oxygen flow rate with a fast-acting valve located in the oxygen supply line just upstream of the injector dome and noting the subsequent change in chamber pressure. In addition, dominant chamber-pressure frequencies were used to calculate approximate dead times corresponding to two different engine dynamic combustion models, and these dead times are compared with the measured dead times.

The injector was of the showerhead square-pattern variety. Gaseous hydrogen was supplied at room temperature, and oxygen was supplied as a liquid at about -320° F. Tests were made over a range of chamber pressures from 45 to 300 pounds per square inch absolute, and over a range of oxidant-fuel ratios varying from approximately 2 to 7.

SYMBOLS

$A,B, \ldots F$	exponents
f_c	calculated combustion frequency, cps
f_o	measured combustion frequency, cps
G	function
H	function
K_1,K_2,K_3	proportionality constants, dimensions as required
O/F	oxidant-fuel ratio
P_c	combustion-chamber pressure, lb/sq in. abs
R_c	combustion-chamber gas constant, ft/°R
T_c	combustion-chamber gas temperature, °R

V_c	combustion-chamber volume, cu ft
v_{LOX}	oxygen injection velocity, ft/sec
w_t	total propellant weight flow, lb/sec
θ_g	gas residence time, sec
σ_c	calculated combustion dead time, corrected for combustion dynamics in terms of gas residence time, millisec
σ_f	calculated combustion dead time from measured frequency data, millisec
σ_o	measured combustion dead time, millisec
φ	phase shift, deg
$\Psi, \Psi_1, \Psi_2, \Psi_3$	functions of time

APPARATUS

Engine

A diagram of the engine used in this investigation is presented in figure 1. The engine was fabricated from 1/2-inch-thick carbon steel and is uncooled. The chamber and the exhaust nozzle are coated with Rokide to minimize overheating damage. The engine is designed to produce 20,000 pounds of thrust at a chamber pressure of 300 pounds per square inch absolute with sea-level nozzle expansion.

Injector

A drawing of the injector is presented in figure 2, showing the orientation, the number, and the diameters of the fuel and oxidant injection orifices. The supplemental fuel holes located around the periphery of the basic square pattern minimize the nonuniformity of the flow caused by the segments formed by the outermost rows of holes and prevent the oxygen from spraying on the engine walls. Fuel holes at the outer lip of the injector faceplate provide film-cooling on the chamber walls during engine operation. The faceplate is concave, having been machined to a 20.0-inch radius; the fuel and oxidant jets are locally perpendicular to the injector face, whereas the cooling holes are arranged for axial discharge.

The fuel and oxidant flow through the injector can be noted from figure 2. The oxidant is supplied to the injector dome, passed directly through the oxygen injection tubes, and discharged into the combustion chamber. Fuel enters the injector at the outer periphery from a separate toroidal-shaped collector and flows around the oxygen injection tubes and through a distribution plate before ejecting into the combustion chamber.

Flow-Disturbance Device

The flow-disturbance device, hereinafter referred to as the "thumper," is a rapidly actuated valve that provides an oxygen flow area decrease of about 20 percent. The desired valve closure time was estimated to be 0.05 millisecond, since the minimum dead time for this engine was estimated to be 0.5 millisecond. A closure time somewhat faster than 0.05 millisecond was obtained with the thumper (patent applied for and information available from NASA Lewis Research Center).

An illustration of the thumper and its components is presented in figure 3; a schematic drawing of the unit is given in figure 4 to show the principles of operation. Oxygen flow is distributed through five ports, one of which is suddenly closed. Each of the ports has provisions for installing variable-sized orifice plates to accommodate the entire oxygen flow range investigated. Flow through the center port passes around a necked-down portion of a piston, so that, when the piston travels, the shaft will close the port and thereby decrease the flow rate. The piston is retained in the cocked position by a ball-release mechanism (see fig. 4), in which eight steel balls are located in a groove in the piston and held by a rotating ring with eight holes. The back side of the piston is pressurized with gaseous nitrogen. When the ring is rotated to aline its eight holes with the balls, the piston is released. The same nitrogen gas used to pressurize the piston is used as a cushion to brake the piston movement at the end of its intended travel.

Figure 5 shows the thumper assembly bolted to the injector dome, which in turn is bolted to the rocket engine on the thrust-measuring stand.

Test Facility

The test cell, the propellant systems, and the exhaust system are described in detail in reference 3. Liquid oxygen was supplied to the engine from the propellant tank by a helium pressure system. The entire oxygen supply line, up to the thumper, is immersed in an open liquid-nitrogen trough to ensure a uniform oxidant temperature through the system. Gaseous hydrogen was supplied to the engine at room temperature from a manifolded bank of high-pressure cylinders.

Instrumentation

Oxygen flow rate was metered with a calibrated Venturi flowmeter located in the oxygen supply tank. Gaseous hydrogen flow was measured with a calibrated ASME flat-plate orifice. Corresponding pressure drops for both the oxidant- and the fuel-flow rates were recorded on self-balancing calibrated potentiometers. Oxidant flowmeter temperature was measured with a platinum-coil resistor; the corresponding fuel temperature was measured with an iron-constantan thermocouple. These temperature measurements were also recorded on potentiometers.

The steady-state chamber-pressure measurement was made with a low-response strain-gage-type transducer from a static-pressure tap located on the injector face. Two pressure-measuring sites are provided on both the injector dome and the combustion chamber in order to obtain the dynamic-pressure readings from which dead time is estimated directly. The measuring sites on the oxygen dome are located near each other and on a radius about $3\frac{1}{2}$ inches from the engine centerline. The measuring sites on the combustion chamber are located about 4 inches downstream of the injector face 90° apart. Commercial high-frequency-response pressure transducers are mounted at each of the four sites. The pressure-sensitive faces of the two transducers on the dome are located flush with the inside surface of the dome. One of the chamber-pressure transducers is installed flush with the Rokide coating of the combustion chamber. The pressure-sensitive face of the second chamber-pressure transducer is located in a hole 3/16 inch from the inside chamber wall. The diameter of this hole immediately reduces to 1/10 inch (see fig. 1) and constitutes the pressure tap. The acoustical resonance of this configuration is calculated to be about 8000 cycles per second, which is well above the 1500-cycle-per-second maximum frequency expected in the combustor. Comparison of chamber-pressure traces from the two transducer installations for the initial tests indicated no differences. Accordingly, in subsequent tests the recessed configuration was used for both chamber-pressure transducers, thereby considerably reducing the transducer cooling requirements.

Data from these four transducers were recorded on magnetic tape using an FM carrier. The data were then played back at reduced tape speed into matched recording galvanometer channels. Filtering of 40 decibels per decade for recorded frequencies greater than 2000 cps was used in each channel to reduce the noise level. In addition to playing the data from the tape into recording galvanometers, the chamber-pressure data were also played at the recorded speed directly into a Brüel-Kjoer frequency spectrum analyser, and the dominant chamber-pressure frequencies were thus obtained.

PROCEDURE

Because the rocket engine was uncooled, test runs were limited to approximately 4 seconds. Stable rocket-engine operating conditions were attained about 1/2 second after engine start. Midway in the stable portion of each run, the thumper was actuated, thereby reducing the oxygen flow by about 20 percent. This operation produced effectively two sets of data for each engine run, because the oxygen-fuel ratio, and hence engine operating conditions, are changed from the pre-thump to the post-thump portions of the run.

Test points were selected to cover a range of oxidant-fuel ratios from 2 to 7 at various chamber pressures ranging from 45 to 300 pounds per square inch absolute.

The pressure traces for a representative run (P_c = 62.2 lb/sq in. abs) are shown in figure 6. Two chamber-pressure traces and one oxygen-dome pressure trace are indicated. The second dome pressure trace was not recorded because of malfunction of the transducer. Each major time division on figure 6 represents 1/80 second, and each subdivision of time represents 1/800 second, or 1.25 milliseconds. Combustion dead time is defined herein as the elapsed time for a perturbation in the dome pressure to be observed in the combustion-chamber pressure as the oxygen flow is decreased by the thumper. For the traces shown in figure 6, it appears that the dome pressure perturbation occurs at point A, and the chamber pressure responds at either point B or C, depending on the observer's opinion. The dead time for this run, then, can be construed as being somewhere between 1.75 and 2.25 milliseconds. Three observers independently read each data point; and, where differences of opinion resulted, the range of dead-time readings is presented in table I and on the dead-time data plots.

RESULTS AND DISCUSSION

Steady-state experimental values of chamber pressure, propellant mass-flow rates, and the attendant oxygen-fuel ratios are presented for all data points in table I. Also included in the table are chamber-pressure frequency and oscillation amplitude data, as well as the observed combustion dead-time data, when measurable. These measured dead times are plotted in figure 7 as a function of the chamber pressure, the number in the symbols indicating the corresponding data point listed in table I. The measured combustion dead times ranged from a minimum of 0.25 millisecond to a maximum of 2.25 milliseconds, with a general and broad trend of decreasing dead time with increasing chamber pressure.

The spread of dead-time data for a constant chamber pressure indicates that some engine variable (or variables) other than chamber

pressure affects the combustion dead time. In addition to analyzing these dead-time data for trends with other engine parameters, the chamber-pressure frequency data were studied, the object being to relate the two sets of data. If a relation can be established, then combustion dead times can be obtained with a combustion-chamber pressure transducer, rather than by resorting to complex equipment such as used herein.

Chamber-pressure frequency measurements were one of the more precise measurements obtained in the present investigation. More frequency data were obtained than dead-time data because (1) not all runs produced a measurable dead time, and (2) two sets of frequency data were obtained for each run (i.e., pre- and post-step). The measured frequencies are presented in table I and are plotted in figure 8 as functions of chamber pressure. Again the numbers within the symbols correspond to the data points listed in table I. Figure 8 shows that the observed frequencies f_o ranged from 250 to 700 cycles per second, with a broad trend of increasing frequency with increasing chamber pressure. As was found for the measured dead-time data of figure 7, the frequency data of figure 8 indicate that other engine parameters must be considered to account for the data band.

Data for the plots of either time variable (σ_o or f_o) as a function of chamber pressure (figs. 7 and 8) were obtained over a range of oxidant-fuel ratio and therefore a range of propellant injection velocities. Most theorists concur that combustion dead time may be related to propellant injection velocities through propellant drop sizes, evaporation rates, and chemical kinetics. Because gaseous hydrogen was used in the experiments, combustion dead time would logically depend upon the oxygen vaporization process. Hence, the oxygen velocity v_{LOX} and the oxidant-fuel ratio were investigated along with the chamber pressure to explain the broad trends of the data exhibited in figures 7 and 8. The combustion dead time and/or the observed frequency can, then, be considered as functions of these three parameters, and an equation can be written symbolically as follows:

$$\Psi = G(P_c, v_{LOX}, O/F) \tag{1}$$

Any two of the three functional variables on the right side of equation (1) are independent, the third being dependent. Equation (1) can then be written in terms of independent variables to produce the following set of three equations:

$$\Psi_1 = H_1(P_c, v_{LOX}) \tag{2}$$

$$\Psi_2 = H_2(P_c, O/F) \tag{3}$$

$$\Psi_3 = H_3(v_{LOX}, O/F) \tag{4}$$

For data analysis purposes, these time functions were considered to be the product of the dependent variables, each raised to an exponent. The preceding equations are respectively rewritten, then, as follows:

$$\Psi_1 = K_1 P_c^A v_{LOX}^B \tag{5}$$

$$\Psi_2 = K_2 P_c^C (O/F)^D \tag{6}$$

$$\Psi_3 = K_3 v_{LOX}^E (O/F)^F \tag{7}$$

The exponents and constants for these equations were determined by a least-squares curve fit by using the arithmetical mean of the dead times for the data points of figure 7 along with the associated values of chamber pressure, oxygen injection velocity, and O/F from table I. As a result, the following set of three equations was evolved:

$$\sigma_o = 0.05272\ P_c^{-1.930} v_{LOX}^{1.445} \tag{8}$$

$$\sigma_o = 0.004000\ P_c^{-0.460} (O/F)^{0.570} \tag{9}$$

$$\sigma_o = 0.001818\ v_{LOX}^{-0.440} (O/F)^{0.709} \tag{10}$$

From these equations, lines of constant values of v_{LOX} and O/F were computed and are shown in figure 9. This figure shows that measured dead time decreased with increasing chamber pressure at constant oxidant-fuel ratio or liquid-oxygen injection velocity. It also shows that the dead time decreased with decreasing O/F at constant chamber pressure or oxygen injection velocity.

From the root-mean-square data calculations, deviation values of +1.31 and -0.69 were obtained, meaning that 68 percent of the measured dead-time data points lie within a range of ±31 percent of their calculated values. An iterative least-squares process, using either the minimum, the maximum, or the mean measured dead-time value for each data point, will halve this deviation. However, the resultant equations were not significantly altered. The deviation can be attributed to both the experimental accuracy in obtaining direct dead-time measurements from pressure traces and to the inherent difficulty of metering the liquid-oxygen flow rate.

In order to obtain some characteristic dead time from frequency measurements, a combustion model must be assumed. Although many models were investigated, the details of two will be presented, one in which

the dead time is considered to be equal to the inverse of twice the observed chamber-pressure frequency ($\sigma_f = 1/2f_o$), and the second in which combustion-chamber gas dynamics were accounted for by appropriate modifications to the observed frequencies. If, for the second model, the chamber pressure is assumed to be uniform at any instant of time, then the response of the chamber pressure following the dead time can be characterized as a first-order lag system with a time constant equal to the gas residence time θ_g. To cause sustained oscillation in a linear system that has a feedback proportional to the output, the system must cause its output signal to be out of phase (180°) with its input signal. The source of this phase shift is the sum of the phase shifts of each time-dependent element in the system. The combustion-chamber-pressure phase shift φ at any frequency is due to the first-order system time dependency of chamber pressure and can be calculated as follows (ref. 4):

$$\varphi = \tan^{-1} 2\pi f_o \theta_g \tag{11}$$

where

$$\theta_g = \frac{V_c P_c}{12 R_c T_c w_t} \tag{12}$$

Theoretical values of R_c and T_c for each experimental data point tabulated in table I were obtained with use of reference 5.

By inserting the experimentally measured chamber-pressure frequency f_o into equation (11) and subtracting this amount of phase shift from the total phase shift (180°), a calculated frequency f_c, chargeable to combustion dead time, can be computed as follows:

$$f_c = \frac{180}{180 - \varphi} f_c \tag{13}$$

This calculated frequency is the frequency at which the linearized engine model will sustain oscillation if the 180° phase shift is chargeable solely to the dead time. Values for dead time corrected for chamber dynamics σ_c can then be computed by using the mathematical relation between dead time and frequency, $\sigma_c = 1/2f_c$. Computed values of σ_c and σ_f are tabulated in table I.

The frequency data for the two combustion models were individually applied in least-squares fits to the basic time-dependent equations (5), (6), and (7), and the constants and exponents were determined. The resulting equations were then converted in terms of appropriate dead times by the aforementioned mathematical relation. With the first model, the following set of three equations results:

$$\sigma_f = 0.04374\ P_c^{-1.640} v_{LOX}^{1.184} \tag{14}$$

$$\sigma_f = 0.005640\ P_c^{-0.424} (O/F)^{0.372} \tag{15}$$

$$\sigma_f = 0.002794\ v_{LOX}^{-0.412} (O/F)^{0.489} \tag{16}$$

The corresponding equations for the second model are

$$\sigma_c = 0.05376\ P_c^{-1.745} v_{LOX}^{1.204} \tag{17}$$

$$\sigma_c = 0.006662\ P_c^{-0.509} (O/F)^{0.381} \tag{18}$$

$$\sigma_c = 0.002875\ v_{LOX}^{-0.494} (O/F)^{0.521} \tag{19}$$

The statistical deviations for the preceding six equations were on the order of ±10 percent, indicating a better data accuracy than observed for the measured dead-time data σ_o. However, about three times as many frequency data points were available for analysis as were measured dead times.

To compare the dead-time results obtained from the two combustion models with those obtained for the measured dead times, grid lines of constant values for v_{LOX} and O/F were established from the appropriate sets of equations. Intersecting grids were again obtained, similar to those shown in figure 9. Although these grids are not shown in their entirety, the parallelogram shapes, obtained from the experimental limits of v_{LOX} (15 and 100 ft/sec) and O/F (2 and 7), are presented in figure 10, along with the corresponding limits for the measured dead-time data. It can be noted that reasonable agreement, particularly in the low-chamber-pressure regime, existed between the measured dead time (σ_o) and the dead time calculated directly from frequency data (σ_f, model 1). When combustion-chamber gas dynamics were accounted for in the determination of dead time through frequency data (σ_c, model 2), good agreement with the measured dead-time data was obtained over the entire range of chamber pressures investigated. This degree of correlation can also be noted by comparing the calculated with the measured dead-time values, all of which are listed in table I.

From the comparisons of figure 10, it can be concluded that the combustion dead time, for control purposes, can adequately be approximated from chamber-pressure frequency measurements. Best agreement of frequency data with measured dead-time data was obtained when combustion-chamber gas residence time was taken into account.

Because dead time was found to be affected by chamber pressure and oxygen injection velocity, perhaps more sophisticated combustion models, such as discussed in references 1, 2, and 6, might have been investigated. These models, however, involve more complex computations, and require inclusion of feed-system characteristics, pressure drops, pressure levels, and other considerations. It is felt that utilization of the more sophisticated models is unwarranted in view of the degree of correlation obtained with the relatively simple model where combustion-chamber gas dynamics were compensated for in the frequency measurements.

SUMMARY OF RESULTS

Experiments were conducted on an uncooled 20,000-pound-thrust gaseous-hydrogen and liquid-oxygen rocket engine over a range of chamber pressure from 45 to 300 pounds per square inch absolute and oxidant-fuel ratio from 2 to 7. Combustion dead times were measured and compared with dead times calculated from frequency data for two assumed combustion models. The following results were obtained:

1. Measured combustion dead time decreased with increasing chamber pressure at constant oxidant-fuel ratio or liquid-oxygen injection velocity. This dead time also decreased with oxidant-fuel ratio at constant chamber pressure or oxygen injection velocity.

2. For the engine model where combustion dead time was considered to be the inverse of twice the measured chamber-pressure frequency, only a fair agreement with the measured dead time was obtained over the range of engine variables investigated.

3. When the measured chamber-pressure frequencies were corrected for gas-dynamics effects in terms of the gas residence time, close agreement with the measured dead times was obtained over the entire range of variables investigated.

CONCLUSION

The combustion dead time, as required for control purposes, can either be measured directly or can be closely approximated from chamber-pressure frequency measurements, if these measurements are corrected for engine dynamics in terms of the gas residence time.

Lewis Research Center
National Aeronautics and Space Administration
Cleveland, Ohio, March 10, 1961

REFERENCES

1. Crocco, Luigi, and Cheng, Sin-I: Theory of Combustion Instability in Liquid Propellant Rocket Motors. Agardograph 8, Butterworth Sci. Pub. (London), 1956.

2. Hurrell, Herbert G.: Analysis of Injection-Velocity Effects on Rocket Motor Dynamics and Stability. NASA TR R-43, 1959.

3. Rothenberg, Edward A., Kutina, Frank J., Jr., and Kinney, George R.: Experimental Performance of Gaseous Hydrogen and Liquid Oxygen in Uncooled 20,000-Pound-Thrust Rocket Engines. NASA MEMO 4-8-59E, 1959.

4. Chestnut, Harold, and Mayer, Robert W.: Servomechanisms and Regulating System Design. Vol. I. John Wiley & Sons, Inc., 1951.

5. Gordon, Sanford, and McBride, Bonnie J.: Theoretical Performance of Liquid Hydrogen with Liquid Oxygen as a Rocket Propellant. NASA MEMO 5-21-59E, 1959.

6. Scala, Sinclaire M.: Transverse Wave and Entropy Wave Combustion Instability in Liquid Propellant Rockets. Ph. D. Thesis, Princeton Univ., 1957.

TABLE I. - PERTINENT TEST RESULTS

Data point	Chamber pressure, P_c, lb/sq in. abs	Oxygen flow rate, lb/sec	Hydrogen flow rate, lb/sec	Oxidant-fuel ratio, O/F	Observed chamber-pressure frequency, f_c, cps	Observed combustion dead time, σ_o, millisec	Calculated combustion dead time		Calculated oxygen injection velocity, v_{LOX}, ft/sec	Oscillation amplitude, % steady state	Fundamental and/or harmonics present in order of strength	Associated pre-disturbance point
							σ_f, millisec	σ_c, millisec				
1	45	6.43	2.79	2.30	300	---------	1.67	1.43	12.73	28	1,3,5	--
2	50.8	8.68	2.09	4.15	---	1.0-1.25	----	----	17.19	----	-----	--
3	52.4	9.35	1.40	6.68	250	---------	2.00	1.69	18.51	?	0	--
4	53	7.19	2.58	2.79	---	1.25-1.75	----	----	14.24	----	-----	--
5	57.0	9.81	1.62	6.06	270	---------	1.85	1.56	19.42	30	0	9
6	57.2	9.90	1.61	6.15	265	---------	1.89	1.59	19.60	30	0	--
7	58.6	9.27	2.05	4.52	275	---------	1.82	1.55	18.36	40	0,1,2	10
8	61.5	7.31	2.56	2.86	325	---------	1.54	1.34	14.47	50	0,1	11
9	62.2	11.11	1.84	6.77	250	1.75-2.25	2.00	1.69	22.00	0-5	0	--
10	64.6	10.84	2.06	5.26	290	---------	1.72	1.44	21.46	20	0,1,2	--
11	67.0	10.03	2.55	3.93	330	---------	1.52	1.27	19.86	50	0,1	--
12	70	9.86	4.40	2.24	325	---------	1.54	1.35	19.52	50	0,1,2	13
13	78	11.28	4.50	2.51	425	---------	1.18	.96	22.33	50	0,1,2	--
14	98	15.35	3.89	4.16	410	---------	1.22	.97	30.39	?	0,1	16
15	102	17.18	3.05	5.83	360	---------	1.39	1.11	34.02	0	0	17
16	110	18.18	3.71	4.90	320	---------	1.56	1.29	36.00	?	0,1	--
17	112	20.73	3.11	6.67	290	1.0-1.2	1.72	1.42	41.05	0	0	--
18	124	16.21	7.32	2.21	480	---------	1.04	.84	32.10	35	0	20
19	134	20.20	6.55	3.08	555	---------	.90	.68	40.00	60	0,1	23
20	137	19.41	7.51	2.58	560	.68	.89	.68	36.45	24	0	--
21	141	25.62	4.31	5.94	390	---------	1.28	1.00	50.73	4	2	25
22	142	24.68	5.26	4.69	380	---------	1.32	1.04	48.83	24	0	26
23	155	23.9	8.82	3.50	460	.50-.88	1.09	.85	47.32	55	0	--
24	155	31.06	3.49	8.90	---	.90-1.10	----	----	61.50	----	-----	--
25	159	30.1	4.36	6.90	390	1.35-1.60	1.28	.99	59.60	4	2	--
26	166	28.46	5.34	5.33	385	.75-1.00	1.30	1.03	58.35	3	0	--
27	179	30.21	6.29	4.80	400	---------	1.25	.99	59.82	5-10	0,3,5	32
28	185	25.47	11.17	2.28	890	---------	.72	.54	50.43	0-5	0,1	33
29	198.2	27.78	10.33	2.89	580	---------	.86	.66	54.97	0-5	0,1	34
30	201	28.94	10.66	2.71	590	---------	.85	.64	57.30	50	0,1	35
31	203	34.72	7.12	4.88	---	1.06-1.31	----	----	68.75	----	-----	--
32	207	35.17	6.58	5.34	410	.88-1.12	1.22	.96	69.64	5	0,3,5	--
33	218.7	29.29	11.60	2.53	680	.50-.75	.74	.55	58.00	0-5	0,1	--
34	220.9	32.95	10.62	3.10	570	.25-.58	.88	.66	65.24	0-5	0	--
35	222	33.09	11.06	2.99	610	---------	.82	.61	65.52	42	0,1	--
36	222	31.98	10.54	3.03	590	---------	.85	.64	63.32	42	0	37
37	253	38.09	10.88	3.50	575	.38-.75	.87	.66	75.32	5	0	--
38	257.4	37.89	12.79	2.96	590	---------	.85	.64	75.03	0-10	0,1	41
39	282	41.85	10.07	4.14	570	---------	.88	.65	82.47	0-5	0	42
40	288.4	44.51	11.56	3.85	---	.38-.50	----	----	88.13	----	-----	--
41	289.4	43.47	14.52	2.99	600	.80-1.00	.83	.62	86.07	0-5	0,1	--
42	294	48.42	10.54	4.59	570	---------	.88	.65	95.88	0-5	0	--

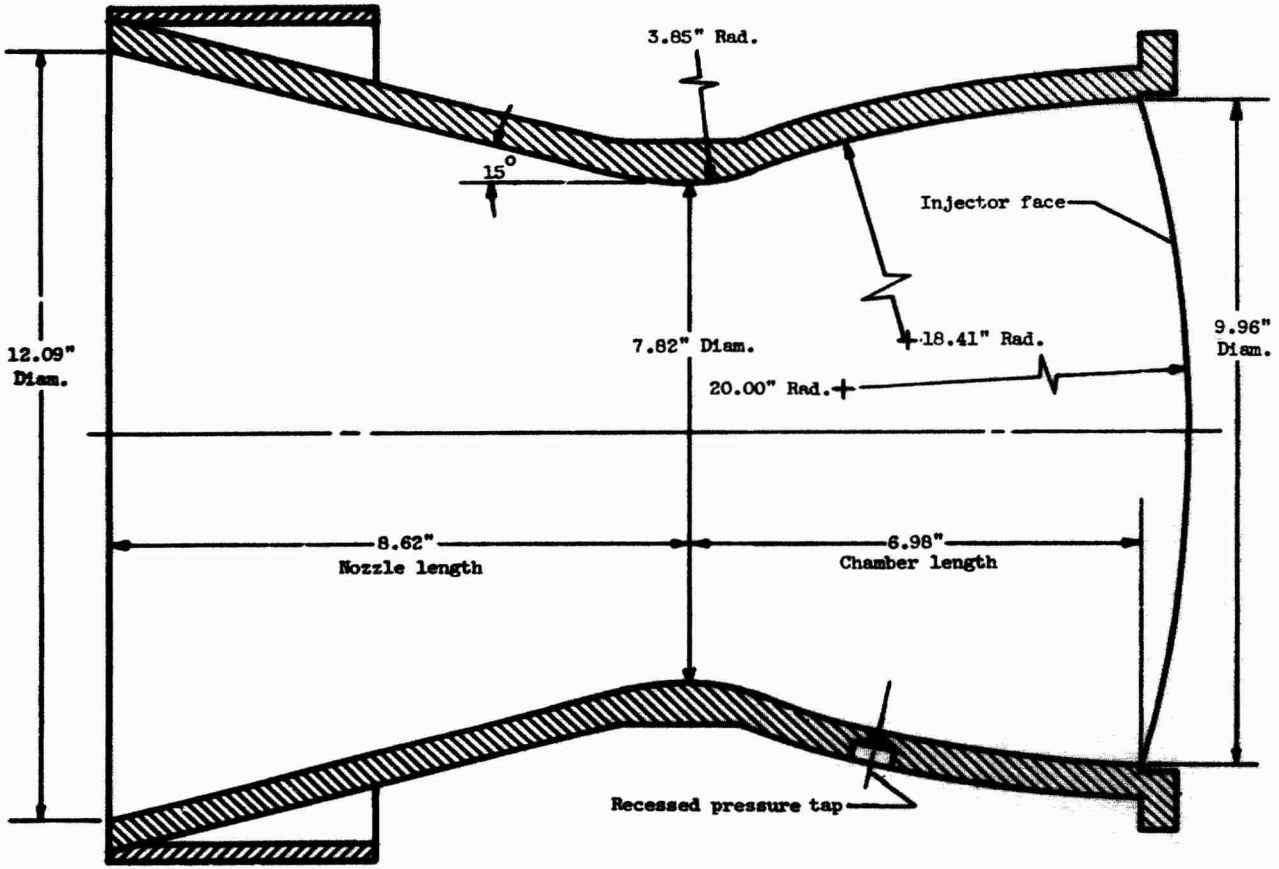

Figure 1. - Uncooled rocket thrust chamber for 20,000-pound thrust, chamber pressure of 300 pounds per square inch absolute, and sea-level expansion.

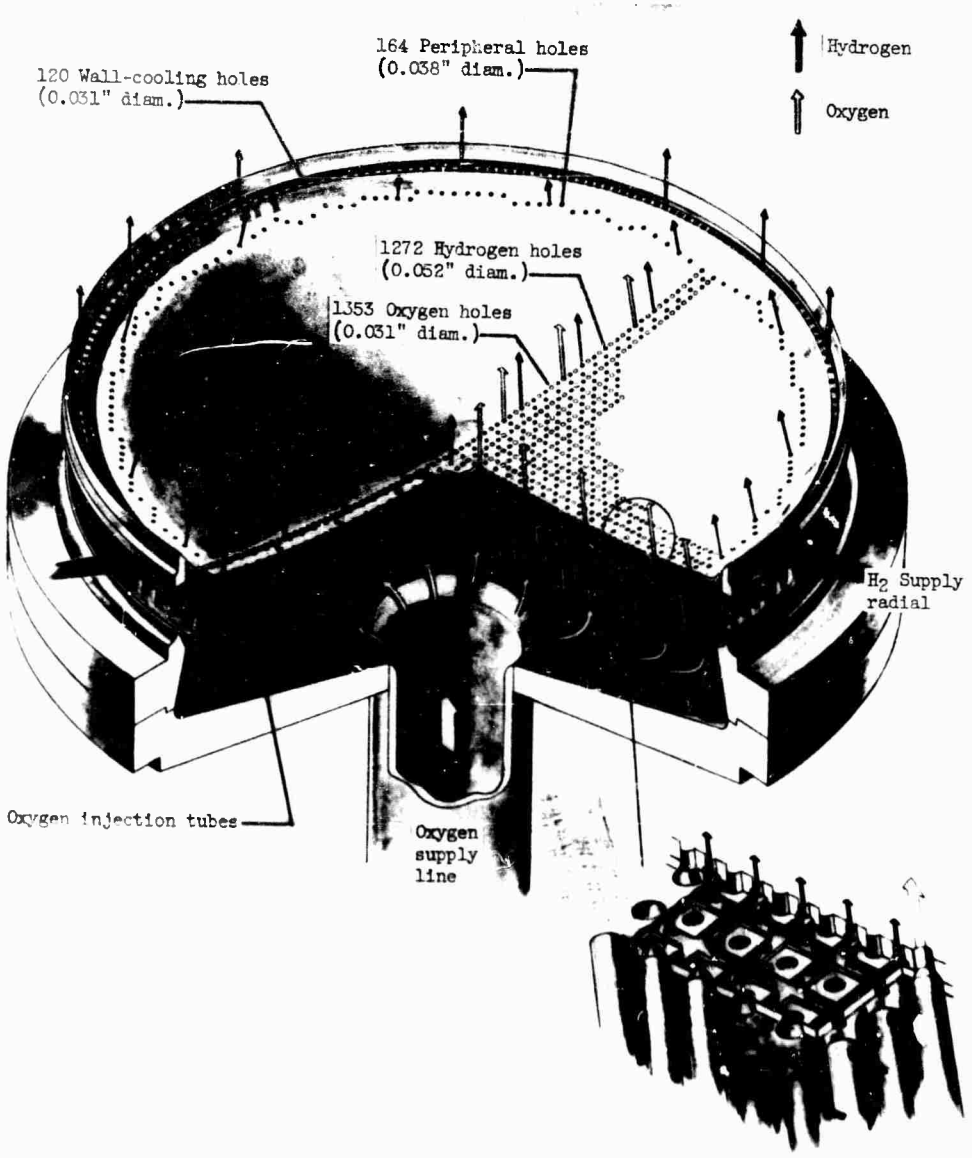
Hydrogen
Oxygen
164 Peripheral holes
(0.038" diam.)
120 Wall-cooling holes
(0.031" diam.)
1272 Hydrogen holes
(0.052" diam.)
1353 Oxygen holes
(0.031" diam.)
H_2 Supply
radial
Oxygen injection tubes
Oxygen
supply
line

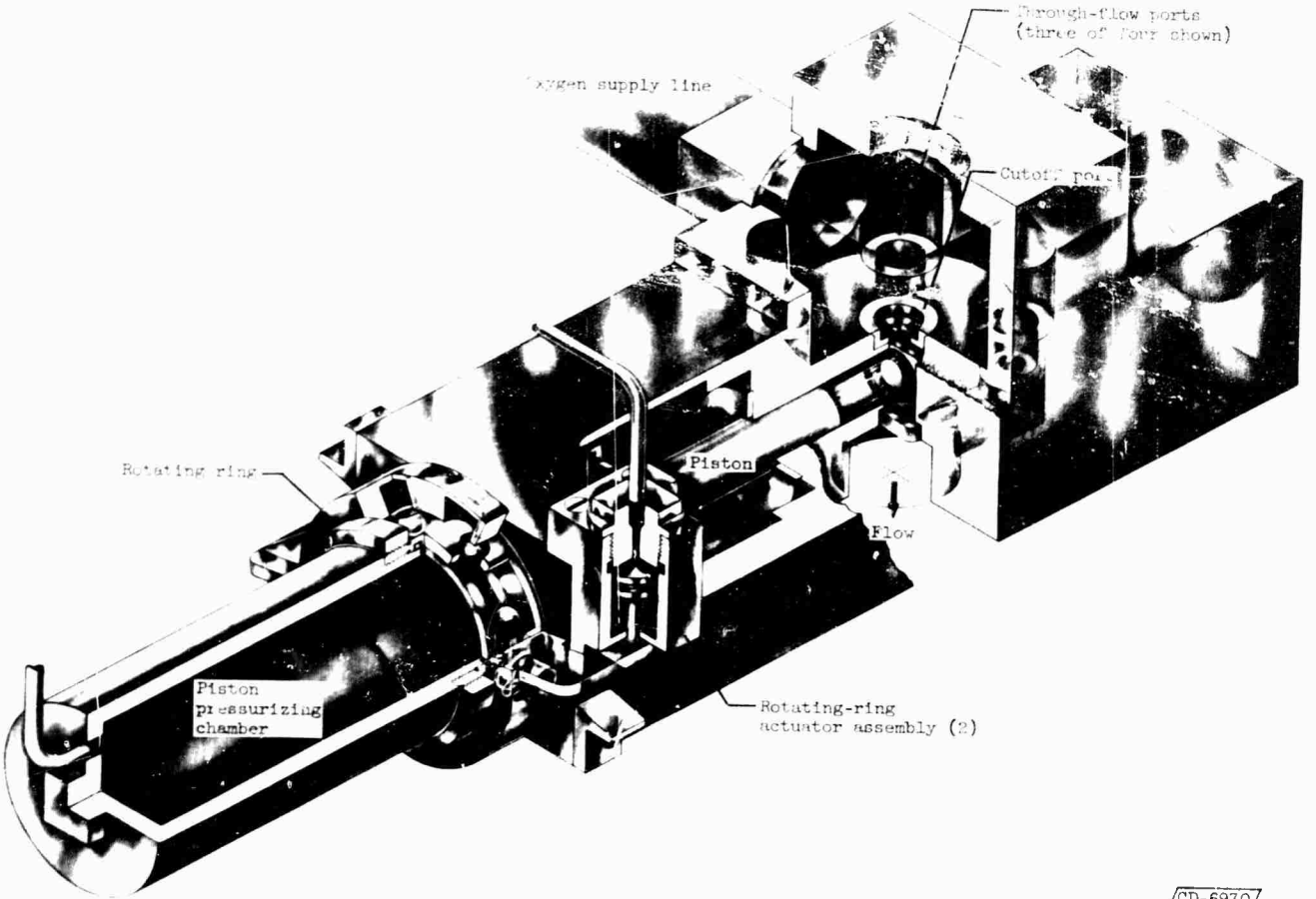
Through-flow ports
(three of four shown)
Oxygen supply line
Cutoff port
Rotating ring
Piston
Flow
Piston
pressurizing
chamber
Rotating-ring
actuator assembly (2)
CD-6970

Figure [illegible]

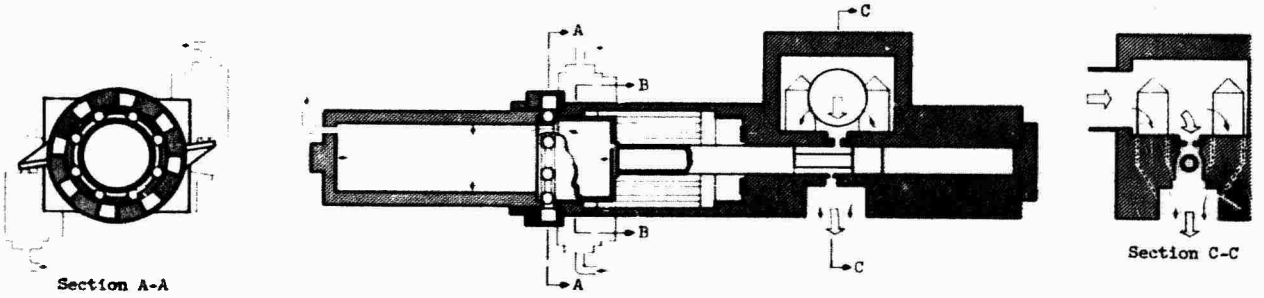

(a) Piston in cocked position.

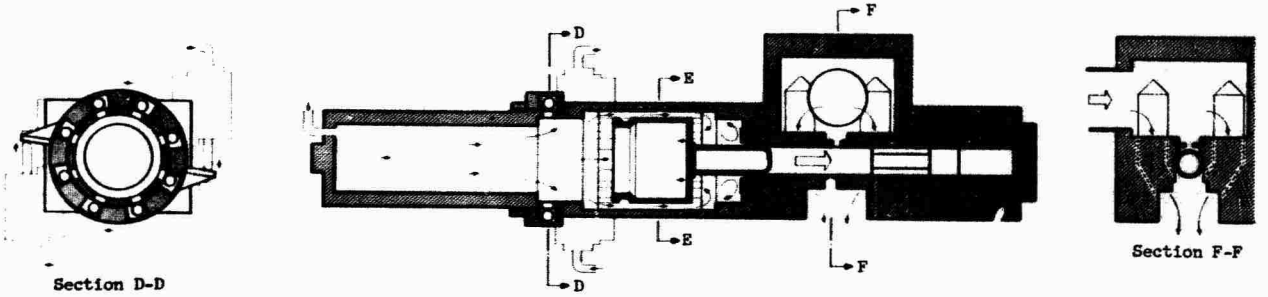

(b) Piston in released position.

Figure 4. - Schematic drawing of thumper in cocked and released positions.

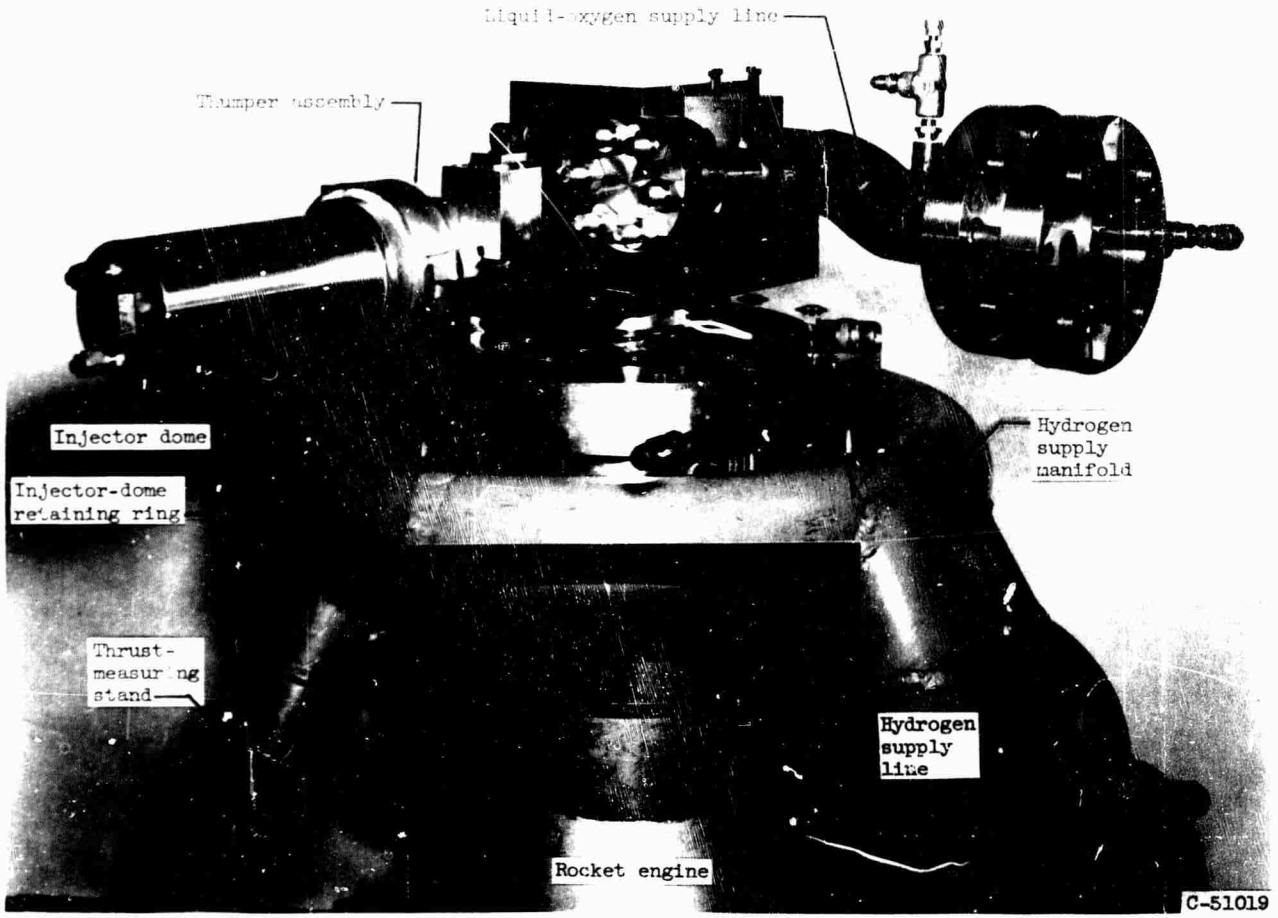

Figure 1. - Assembly of thumper, injector, engine, and thrust stand.

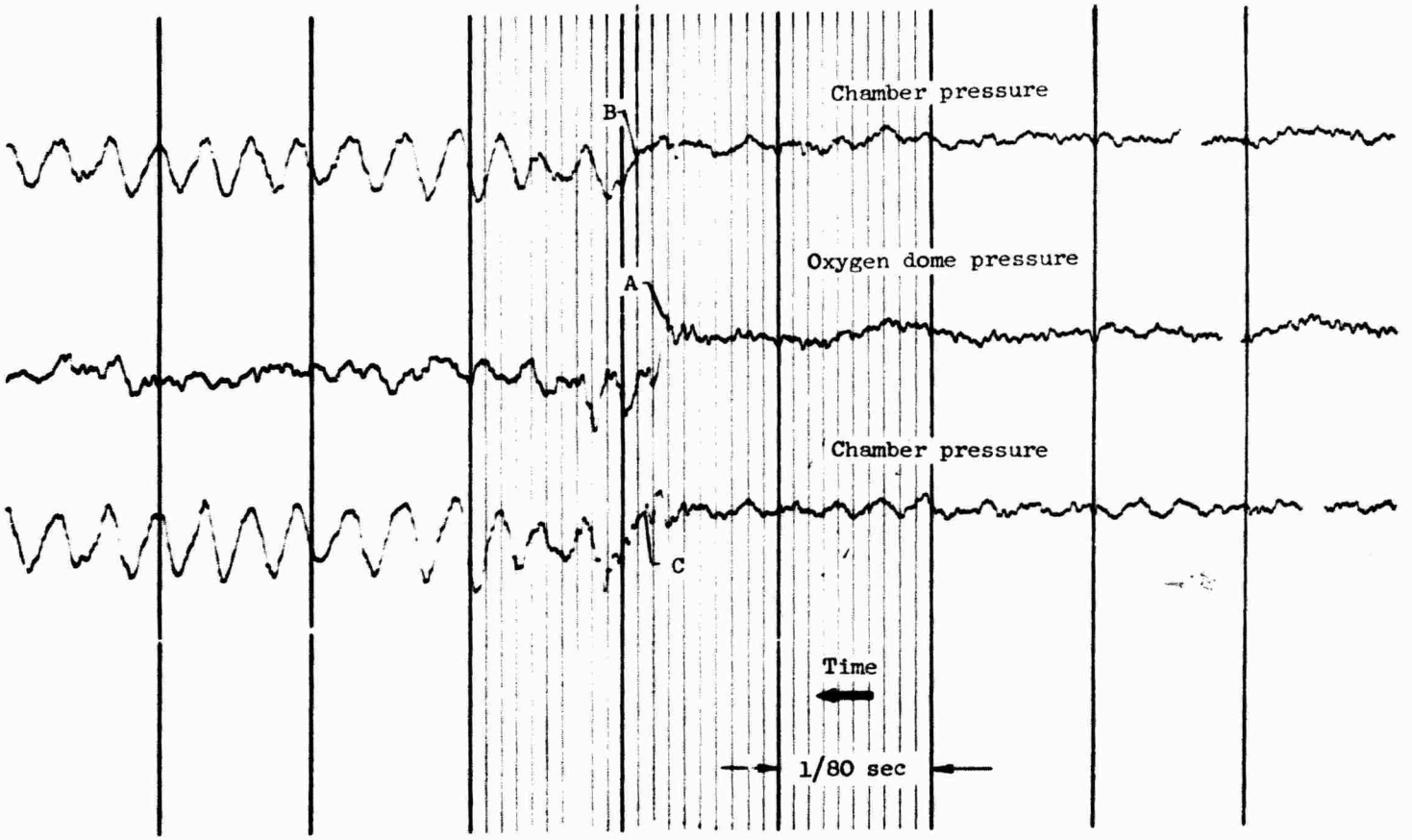

Figure 6. - Pressure traces for representative step disturbance (data point 9).

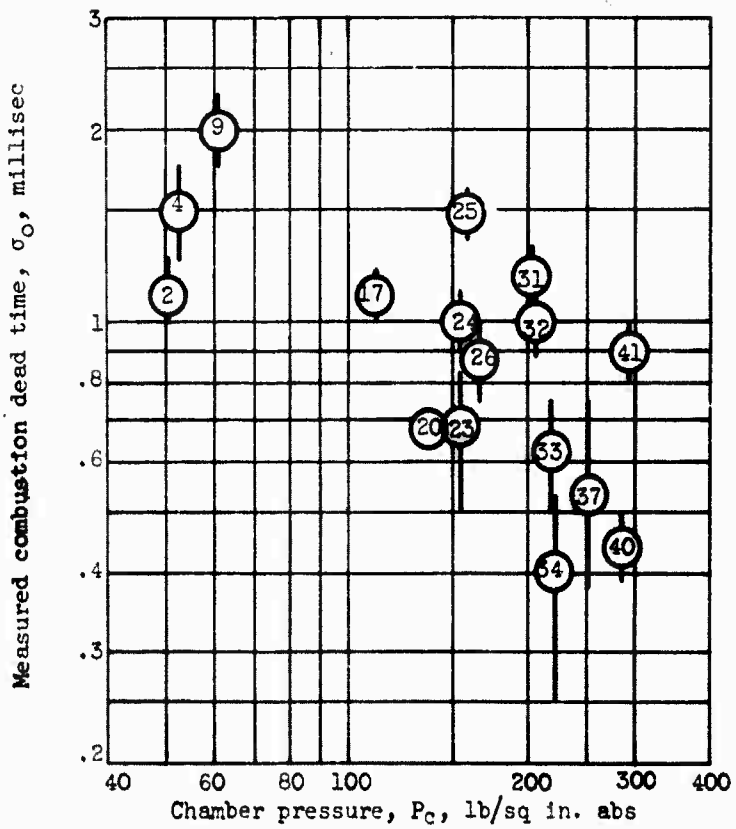

Figure 7. - Measured dead times as function of chamber pressure.

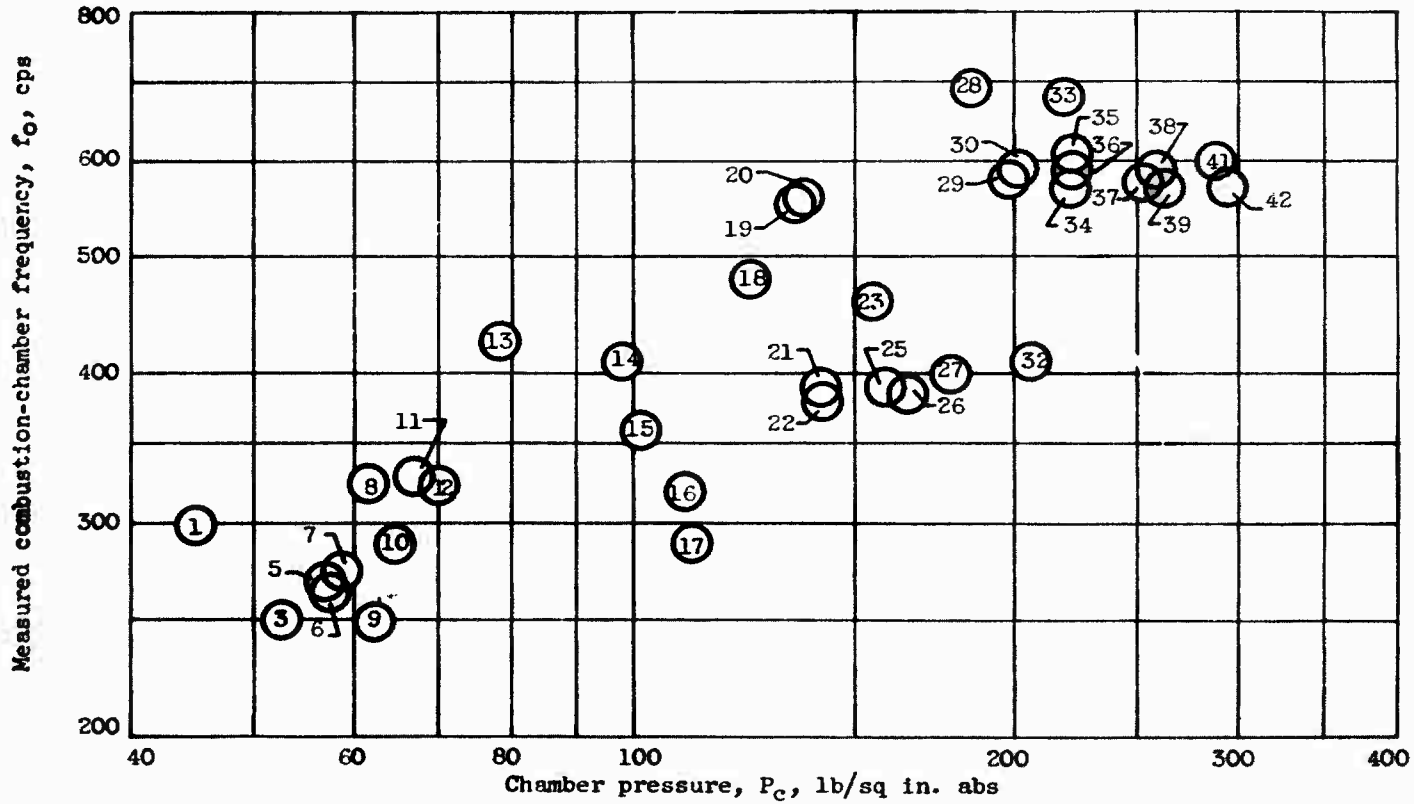

Figure 8. - Measured combustion frequency as function of chamber pressure.

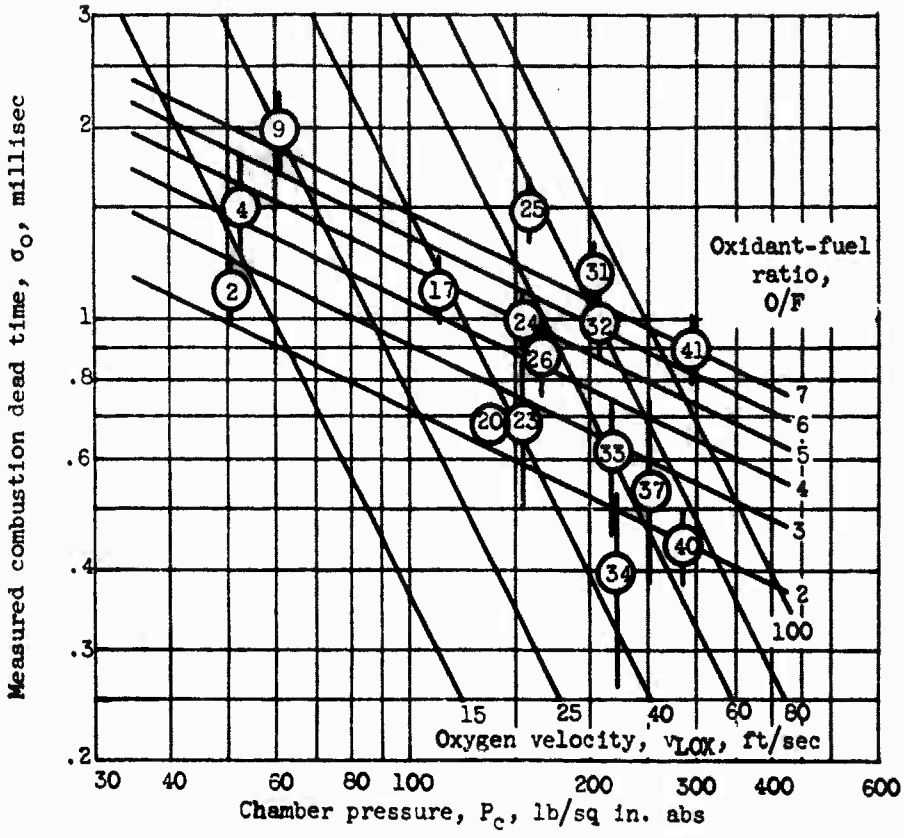

Figure 9. - Measured combustion dead time as function of chamber pressure with lines of oxygen injection velocity and oxidant-fuel ratio calculated from equations (8) to (10).

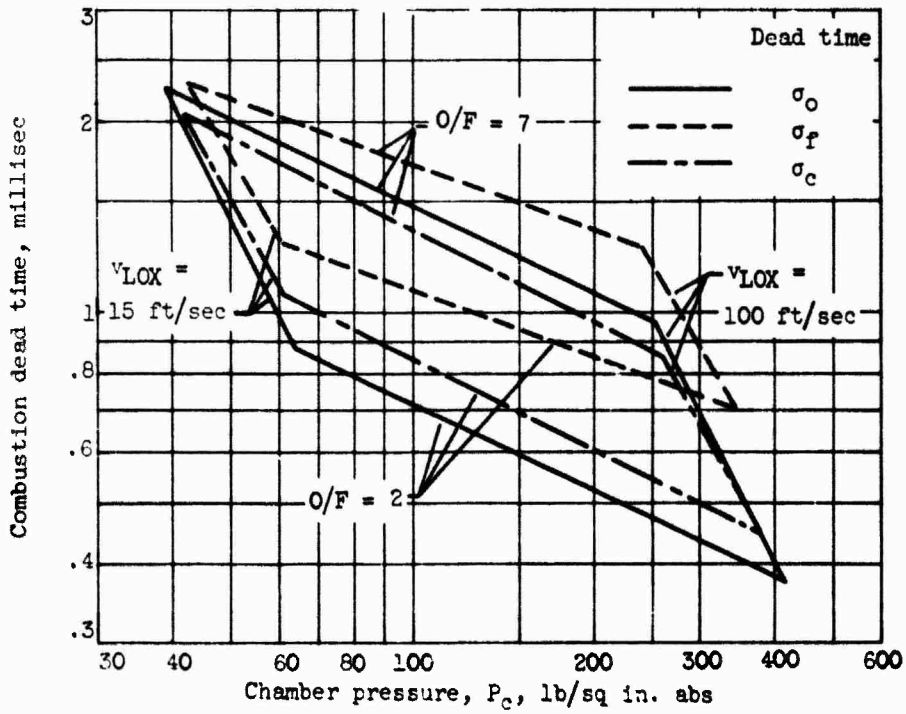

Figure 10. - Intersecting grid limits for three different dead-time determinations.

NASA TN D-851
National Aeronautics and Space Administration.
RELATIONS OF COMBUSTION DEAD TIME TO ENGINE VARIABLES FOR A 20,000-POUND-THRUST GASEOUS-HYDROGEN - LIQUID-OXYGEN ROCKET ENGINE. Daniel I. Drain, Harold J. Schum, and Charles A. Wasserbauer. June 1961. 23p. OTS price, $0.75. (NASA TECHNICAL NOTE D-851)

The time for combustion pressure P_c to respond to an abrupt change in oxygen flow rate, called dead time σ, was measured over a range of P_c from 45 to 300 psia and O/F from 2 to 7. Also, P_c frequencies f were measured and several combustion models were analyzed in which σ was calculated from f. By adjusting the measured f for effect of gas residence time and by considering σ to be the inverse of twice this adjusted f, good agreement was obtained between measured and calculated σ. The σ were correlated with P_c in terms of oxygen injection velocity and O/F. Thus, for control

Copies obtainable from NASA, Washington (over)

I. Drain, Daniel I.
II. Schum, Harold J.
III. Wasserbauer, Charles A.
IV. NASA TN D-851

(Initial NASA distribution: 39, Propulsion systems, liquid-fuel rockets; 44, Propulsion systems, theory; 50, Stability and control.)

NASA

NASA TN D-851
National Aeronautics and Space Administration.
RELATIONS OF COMBUSTION DEAD TIME TO ENGINE VARIABLES FOR A 20,000-POUND-THRUST GASEOUS-HYDROGEN - LIQUID-OXYGEN ROCKET ENGINE. Daniel I. Drain, Harold J. Schum, and Charles A. Wasserbauer. June 1961. 23p. OTS price, $0.75. (NASA TECHNICAL NOTE D-851)

The time for combustion pressure P_c to respond to an abrupt change in oxygen flow rate, called dead time σ, was measured over a range of P_c from 45 to 300 psia and O/F from 2 to 7. Also, P_c frequencies f were measured and several combustion models were analyzed in which σ was calculated from f. By adjusting the measured f for effect of gas residence time and by considering σ to be the inverse of twice this adjusted f, good agreement was obtained between measured and calculated σ. The σ were correlated with P_c in terms of oxygen injection velocity and O/F. Thus, for control

Copies obtainable from NASA, Washington (over)

I. Drain, Daniel I.
II. Schum, Harold J.
III. Wasserbauer, Charles A.
IV. NASA TN D-851

(Initial NASA distribution: 39, Propulsion systems, liquid-fuel rockets; 44, Propulsion systems, theory; 50, Stability and control.)

NASA

NASA TN D-851
National Aeronautics and Space Administration.
RELATIONS OF COMBUSTION DEAD TIME TO ENGINE VARIABLES FOR A 20,000-POUND-THRUST GASEOUS-HYDROGEN - LIQUID-OXYGEN ROCKET ENGINE. Daniel I. Drain, Harold J. Schum, and Charles A. Wasserbauer. June 1961. 23p. OTS price, $0.75. (NASA TECHNICAL NOTE D-851)

The time for combustion pressure P_c to respond to an abrupt change in oxygen flow rate, called dead time σ, was measured over a range of P_c from 45 to 300 psia and O/F from 2 to 7. Also, P_c frequencies f were measured and several combustion models were analyzed in which σ was calculated from f. By adjusting the measured f for effect of gas residence time and by considering σ to be the inverse of twice this adjusted f, good agreement was obtained between measured and calculated σ. The σ were correlated with P_c in terms of oxygen injection velocity and O/F. Thus, for control

Copies obtainable from NASA, Washington (over)

I. Drain, Daniel I.
II. Schum, Harold J.
III. Wasserbauer, Charles A.
IV. NASA TN D-851

(Initial NASA distribution: 39, Propulsion systems, liquid-fuel rockets; 44, Propulsion systems, theory; 50, Stability and control.)

NASA

NASA TN D-851
National Aeronautics and Space Administration.
RELATIONS OF COMBUSTION DEAD TIME TO ENGINE VARIABLES FOR A 20,000-POUND-THRUST GASEOUS-HYDROGEN - LIQUID-OXYGEN ROCKET ENGINE. Daniel I. Drain, Harold J. Schum, and Charles A. Wasserbauer. June 1961. 23p. OTS price, $0.75. (NASA TECHNICAL NOTE D-851)

The time for combustion pressure P_c to respond to an abrupt change in oxygen flow rate, called dead time σ, was measured over a range of P_c from 45 to 300 psia and O/F from 2 to 7. Also, P_c frequencies f were measured and several combustion models were analyzed in which σ was calculated from f. By adjusting the measured f for effect of gas residence time and by considering σ to be the inverse of twice this adjusted f, good agreement was obtained between measured and calculated σ. The σ were correlated with P_c in terms of oxygen injection velocity and O/F. Thus, for control

Copies obtainable from NASA, Washington (over)

I. Drain, Daniel I.
II. Schum, Harold J.
III. Wasserbauer, Charles A.
IV. NASA TN D-851

(Initial NASA distribution: 39, Propulsion systems, liquid-fuel rockets; 44, Propulsion systems, theory; 50, Stability and control.)

NASA

NASA TN D-851

purposes, combustion dead time can be closely approximated from P_c frequency measurements.

Copies obtainable from NASA, Washington

NASA

NASA TN D-851

purposes, combustion dead time can be closely approximated from P_c frequency measurements.

Copies obtainable from NASA, Washington

NASA

NASA TN D-851

purposes, combustion dead time can be closely approximated from P_c frequency measurements.

Copies obtainable from NASA, Washington

NASA

NASA TN D-851

purposes, combustion dead time can be closely approximated from P_c frequency measurements.

Copies obtainable from NASA, Washington

NASA

NASA TN D-851
National Aeronautics and Space Administration.
RELATIONS OF COMBUSTION DEAD TIME TO ENGINE VARIABLES FOR A 20,000-POUND-THRUST GASEOUS-HYDROGEN - LIQUID-OXYGEN ROCKET ENGINE. Daniel I. Drain, Harold J. Schum, and Charles A. Wasserbauer. June 1961. 23p. OTS price, $0.75. (NASA TECHNICAL NOTE D-851)

The time for combustion pressure P_c to respond to an abrupt change in oxygen flow rate, called dead time σ, was measured over a range of P_c from 45 to 300 psia and O/F from 2 to 7. Also, P_c frequencies f were measured and several combustion models were analyzed in which σ was calculated from f. By adjusting the measured f for effect of gas residence time and by considering σ to be the inverse of twice this adjusted f, good agreement was obtained between measured and calculated σ. The σ were correlated with P_c in terms of oxygen injection velocity and O/F. Thus, for control

Copies obtainable from NASA, Washington (over)

I. Drain, Daniel I.
II. Schum, Harold J.
III. Wasserbauer, Charles A.
IV. NASA TN D-851

(Initial NASA distribution: 39, Propulsion systems, liquid-fuel rockets; 44, Propulsion systems, theory; 50, Stability and control.)

NASA

NASA TN D-851
National Aeronautics and Space Administration.
RELATIONS OF COMBUSTION DEAD TIME TO ENGINE VARIABLES FOR A 20,000-POUND-THRUST GASEOUS-HYDROGEN - LIQUID-OXYGEN ROCKET ENGINE. Daniel I. Drain, Harold J. Schum, and Charles A. Wasserbauer. June 1961. 23p. OTS price, $0.75. (NASA TECHNICAL NOTE D-851)

The time for combustion pressure P_c to respond to an abrupt change in oxygen flow rate, called dead time σ, was measured over a range of P_c from 45 to 300 psia and O/F from 2 to 7. Also, P_c frequencies f were measured and several combustion models were analyzed in which σ was calculated from f. By adjusting the measured f for effect of gas residence time and by considering σ to be the inverse of twice this adjusted f, good agreement was obtained between measured and calculated σ. The σ were correlated with P_c in terms of oxygen injection velocity and O/F. Thus, for control

Copies obtainable from NASA, Washington (over)

I. Drain, Daniel I.
II. Schum, Harold J.
III. Wasserbauer, Charles A.
IV. NASA TN D-851

(Initial NASA distribution: 39, Propulsion systems, liquid-fuel rockets; 44, Propulsion systems, theory; 50, Stability and control.)

NASA

NASA TN D-851
National Aeronautics and Space Administration.
RELATIONS OF COMBUSTION DEAD TIME TO ENGINE VARIABLES FOR A 20,000-POUND-THRUST GASEOUS-HYDROGEN - LIQUID-OXYGEN ROCKET ENGINE. Daniel I. Drain, Harold J. Schum, and Charles A. Wasserbauer. June 1961. 23p. OTS price, $0.75. (NASA TECHNICAL NOTE D-851)

The time for combustion pressure P_c to respond to an abrupt change in oxygen flow rate, called dead time σ, was measured over a range of P_c from 45 to 300 psia and O/F from 2 to 7. Also, P_c frequencies f were measured and several combustion models were analyzed in which σ was calculated from f. By adjusting the measured f for effect of gas residence time and by considering σ to be the inverse of twice this adjusted f, good agreement was obtained between measured and calculated σ. The σ were correlated with P_c in terms of oxygen injection velocity and O/F. Thus, for control

Copies obtainable from NASA, Washington (over)

I. Drain, Daniel I.
II. Schum, Harold J.
III. Wasserbauer, Charles A.
IV. NASA TN D-851

(Initial NASA distribution: 39, Propulsion systems, liquid-fuel rockets; 44, Propulsion systems, theory; 50, Stability and control.)

NASA

NASA TN D-851
National Aeronautics and Space Administration.
RELATIONS OF COMBUSTION DEAD TIME TO ENGINE VARIABLES FOR A 20,000-POUND-THRUST GASEOUS-HYDROGEN - LIQUID-OXYGEN ROCKET ENGINE. Daniel I. Drain, Harold J. Schum, and Charles A. Wasserbauer. June 1961. 23p. OTS price, $0.75. (NASA TECHNICAL NOTE D-851)

The time for combustion pressure P_c to respond to an abrupt change in oxygen flow rate, called dead time σ, was measured over a range of P_c from 45 to 300 psia and O/F from 2 to 7. Also, P_c frequencies f were measured and several combustion models were analyzed in which σ was calculated from f. By adjusting the measured f for effect of gas residence time and by considering σ to be the inverse of twice this adjusted f, good agreement was obtained between measured and calculated σ. The σ were correlated with P_c in terms of oxygen injection velocity and O/F. Thus, for control

Copies obtainable from NASA, Washington (over)

I. Drain, Daniel I.
II. Schum, Harold J.
III. Wasserbauer, Charles A.
IV. NASA TN D-851

(Initial NASA distribution: 39, Propulsion systems, liquid-fuel rockets; 44, Propulsion systems, theory; 50, Stability and control.)

NASA

NASA TN D-851

purposes, combustion dead time can be closely approximated from P_c frequency measurements.

Copies obtainable from NASA, Washington

NASA

NASA TN D-851

purposes, combustion dead time can be closely approximated from P_c frequency measurements.

Copies obtainable from NASA, Washington

NASA

NASA TN D-851

purposes, combustion dead time can be closely approximated from P_c frequency measurements.

Copies obtainable from NASA, Washington

NASA

NASA TN D-851

purposes, combustion dead time can be closely approximated from P_c frequency measurements.

Copies obtainable from NASA, Washington

NASA